3D SPATIAL DISTRIBUTION OF BIOPHYSICAL PARAMETERS DERIVED FROM HYPERSPECTRAL AND LIDAR REMOTE SENSING. IMPROVING THE CONSTRAINTS IN LAND SURFACE MODELLING

J.A.J. Berni[a], N. Kljun[b], E. Van Gorsel[a], V. Haverd[a], R .LEUNING[a], A. Cabello-Leblic[a], A. Held[a], C. Hopkinson[c], L. Chasmer[c], K. Youngentob[e]

[a]CSIRO Marine and Atmospheric Research, Canberra, Australia
(jose.jimenez-berni,eva.vangorsel,vanessa.haverd,ray.leuning,arancha.cabello,alex.held@csiro.au)
[b]Swansea University, Swansea, United Kingdom (n.kljun@swansea.ac.uk)
[c]Applied Geomatics Research Group, Lawrencetown NS, Canada (chris.hopkinson@nscc.ca)
[d]Cold Regions Research Centre, Wilfrid Laurier University, Waterloo, ON, Canada (lechasme@yahoo.ca)
[e]The Fenner School of Environment and Society, ANU, Canberra, Australia (kara.youngentob@anu.edu.au)

Abstract - A hyperspectral sensor and a full waveform LiDAR were flown over a temperate *Eucalyptus* forest in Australia, at the location of the Tumbarumba Ozflux site. Ground cover and leaf area index were derived from the LiDAR dataset while chlorophyll content maps were generated from the hyperspectral imagery using 3D radiative transfer models and the structural information derived from the LiDAR. These maps were subsequently used to replace fixed parameters in land surface models (LSM). We used the LSM CABLE-SLI to demonstrate how spatial variability in biophysical parameters translates into changes in net ecosystem exchange. .

Keywords: Carbon Exchange, LiDAR, Hyperspectral, Radiative Transfer Models, biophysical parameters.

INTRODUCTION

A key focus of research in biogeosciences is the net carbon exchange of ecosystems (Running et al, 1999). Such research needs the assessment of CO2 fluxes on time scales from hours to years and across spatial scales of leaves to ecosystems (Baldocchi, 2003).

Two major approaches that can be used to this aim are, a) remote sensing: e.g. the use of simple functions of spectral vegetation indexes (SVI) like NDVI or EVI, which relate gross primary production (GPP) with SVI; b) modelling: e.g. use of land surface models (LSM) that include vegetation dynamics and biogeochemistry at several time scales. LSM parameters are commonly a mixture of data-constrained parameters (e.g. eddy covariance flux data, streamflow and soil moisture data) and fixed parameters (e.g. literature values, soil atlas, plant functional types). We will use remotely-sensed hyperspectral and LiDAR data as spatially highly resolved parameters, as they reflect the natural variability and biophysical attributes of the vegetation more realistically.

Direct observations of carbon exchange (ecosystem scale fluxes measured with the eddy covariance method) are also needed to validate estimates derived from remote sensing and LSM. Due to nonlinearities in LSMs, calculated fluxes will be in error if parameters for the component parameters are simply averaged in proportion to their areal fraction (Wang et al. 2001). However, we hypothesise that the use of source area weighted model output will decrease residuals of modelled and measured fluxes.

Quantitative remote sensing using airborne hyperspectral and LiDAR sensors can provide spatially extensive information in three dimensions about biophysical parameters which are linked directly to physiological processes that control carbon and water exchanges in vegetation. The high spatial resolution of these sensors can deliver maps of these driving factors and appropriately account for disturbance effects or heterogeneity.

We propose the combined use of high spatial resolution hyperspectral imagery and LiDAR data in order to derive fine resolution maps of the LSM input parameters. In this case we will focus in the estimation of the photosynthetic capacity in the form of the maximum carboxylation rate ($V_{cmax,0}$, where $_0$ stands for "normalized to standard temperature") and the potential rate of electron transport ($J_{max,0}$); as well as LAI and fCover as structural parameters related with radiation interception. We have used maps of those parameters into the CABLE-SLI model and generated a map of the net ecosystem exchange (NEE).

MATERIALS

Study area

The study area is situated in Bago State Forest, NSW, Australia 35°39'23.89"S, 148° 9'6.02"E, elevation 1200 m). At the center of the study area is Tumbarumba flux tower which has been operational since 2001 (see van Gorsel et al. these proceedings for further details on the study site). The surroundings of the site have been subject to selective logging and partial logging (selective logging and interspersed clear fell logging of 0.5 ha areas) during the recent past.

Airborne data

A full waveform LiDAR (LMS-Q560, Riegl Laser Measurement Systems GmbH, Austria) and a hyperspectral imager (AISA Eagle, Spectral Imaging Ltd, Finland) were flown over the study site on November 7th and 9th 2009. The instruments were flown and operated by Airborne Research Australia (ARA, Flinders University) on board an Eco-Dimona aircraft, which allows for low flying altitudes and speeds. The hyperspectral sensor acquired 252 spectral bands from 400 to 990nm with approximately 2.5nm of bandwidth (FWHM) and delivered a spatial resolution of 1m at the flight altitude of this flight (400m AGL).

Ground data

At the time of the flight different calibration targets were measured with a field spectroradiometer (ASD Fieldspec Pro, USA).

Hemispheric photos were taken at 30 plots around the tower within a circular area of 1 km radius. At each location five photos were taken. One at a central point and one in 17.5 m distance towards N, E, S and W. The camera was mounted on a tripod with a gimbal at 1.4m height. The camera used is a Nikon Coolpix 950 with a FC-E8 fisheye lens. The images were processed with CANEye V5.0 (Weiss et al, 2004).

METHODS

Hyperspectral and LiDAR processing

The hyperspectral images were corrected atmospherically using the irradiance model SMARTS (Gueymard, 2001) and calculating the reflectance as the ratio between the radiance and the irradiance integrated for the whole hemisphere. The inputs for the model (AOD@500nm and equivalent water content) were retrieved from the AERONET station in Canberra, 100km East of Tumbarumba. The calculated reflectance was compared with field measurements at the time of the flight and the overall spectrum matched well the field measurements except in the atmospheric water absorption band (970nm). For this reason the water content was inverted adjusting the value of the parameter until the error in the reflectance for that band was minimized. The final error in the whole reflectance was 2-3% for the different targets measured with the ASD.

The LiDAR data was processed in ENVI (ITTVIS, USA) using the BCAL LiDAR toolkit. The first step was the classification of the point returns into vegetation and ground returns. The linear filter was used and all the returns higher than 60m were filtered out since they were considered outliers. Once the points are classified, the following raster products were generated: digital terrain model (DTM) of the bare ground; maximum vegetation height; binary map of the vegetation higher that 1m for fractional cover calculation (fCover). The datasets were resampled into a 100x100m^2 grid size for its use into the modelling and for computational reasons.

Radiative Transfer Modelling

The PROSPECT5 (Feret et al., 2008) radiative transfer model (RTM) allows simulating the leaf reflectance and transmittance. Inputs include the leaf cellular structure (N parameter) and the leaf biochemistry e.g. chlorophyll concentration (Ch_{a+b}), carotenids (Car), equivalent water content (Cw) and specific density (Cm).

This model can be coupled to a canopy scale RTM which simulates the light scattering within the canopy. In this case the 3-D *Forest Light Interaction Model* (FLIGHT) was chosen. FLIGHT is based on Monte Carlo ray tracing (MCRT) method as a tool to simulate the radiative transfer in a canopy structure (North, 1996). FLIGHT model inputs consist of: (i) geometric characteristics: shape, height, radius, leaf angle distribution (LAD), leaf area index (LAI) and position of every single crown in the scene as well as trunk diameter (DBH); (ii) spectral signatures: soil-, green leaf-, senescence leaf-, bark spectra; (iii) sun and view zenith and azimuth angles; and (iv) other parameters such as soil roughness, aerosol optical thickness and the number of photons simulated. The output of the model simulation is a multispectral image with a given number of bands. Fig. 1 shows examples of three different FLIGHT simulations corresponding to different values of LAI and Ch_{a+b} concentrations.

In this work, the FLIGHT model was used together with PROSPECT to simulate the canopy reflectance. Average tree density and crown dimension were extracted from the vegetation height image derived from the LiDAR. The solar geometry corresponded to the date and time of the flight (solar zenith=23° and solar azimuth=124°).

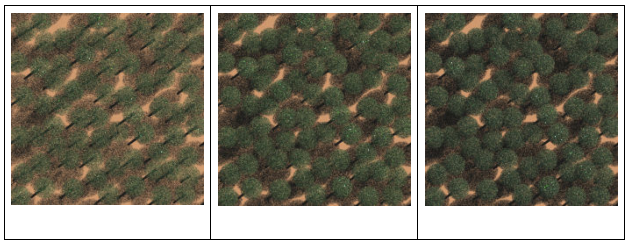

Figure 1. Examples of PROSPECT5+FLIGHT simulations with different input values. a) Ch_{a+b}=30, LAI=1.5; b) Ch_{a+b}=30, LAI=2.5; c) Ch_{a+b}=40, LAI=3

Land surface modelling

CABLE-SLI was chosen as the land surface model used in this study. This model is a combination of CABLE (Community Atmosphere Biosphere Land Exchange model, (Wang et al., *in press*) and SLI (Soil-Litter-Iso). CABLE combines a two-leaf, sun-shade canopy model developed by Wang and Leuning (1998), a model for surface roughness and aerodynamic resistance developed by Raupach et al (1997). Litter-Iso is a one dimensional model for coupled transport of heat, water and stable isotopes in soil with a litter layer and root extraction (Haverd and Cuntz, 2010).

RESULTS AND DISCUSSION

A total number of 944 simulations of PROSPECT5+FLIGHT were created from the combination of parameters shown in Table A. The values were selected for a range of previously studied eucalypt species (Barry et al,).

Table A. Nominal values of the input parameters used in the simulations of FLIGHT+PROSPECT

PROSPECT INPUTS

Leaf Structural Parameter	N	1.45,1.7,1.95
Chlorophyll a+b concentration (µg/cm^2)	Ch_{a+b}	20,23.3,26.7,30 ,33.3,36.7,40
Carotenoids concentration (µg/cm^2)	Car	7.5,10,12.5
Equivalent water content (cm)	C_w	0.017
Leaf dry matter content (g/cm^2)	C_m	0.017

FLIGHT INPUTS

Crown dimensions (m)	5.5,3.5,12.5
fCover	0.7
LAI	1,1.5,2,2.5,3
DBH (m)	0.9
Solar Zenith Angle (º)	26.9
Solar Azimuth (º)	127
Bands (nm)	490,550,670,710,750,800

The simple ratio of the reflectance at 750 and 710nm respectively (ρ750/ρ710) is recognized as good indicator of chlorophyll content at leaf level (Zarco-Tejada et al., 2001), however that index is highly affected by structural effects and doesn't perform equally well at canopy level. In order to assess the effects of the structure in this index, the spectra resulting from the simulation of PROSPECT+FLIGHT were compared with the input value of Ch_{a+b} (figure 2). The index shows a very good linear relationship between Cab and ρ750/ρ710, however different values of LAI have a different slope and intercept. The result therefore is a family of regressions with the following equation:

$$Ch_{a+b} = a\frac{\rho 750}{\rho 710} + b \qquad (1)$$

Where *a* and *b* are functions of the LAI.

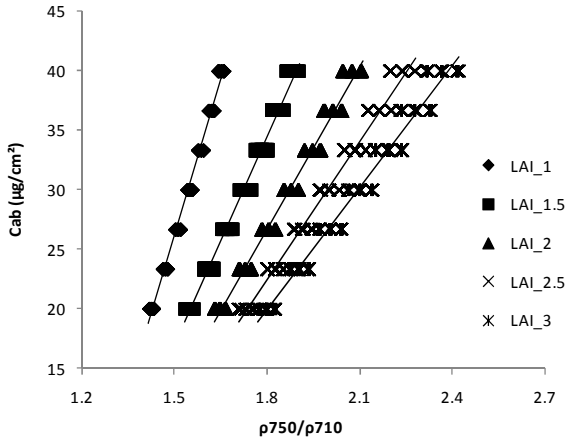

Figure 2. Relationships between the simulated reflectance ρ750/ρ710 and Ch_{a+b} for different LAI values.

The terms *a* and *b* both exponentially decrease with LAI. (figure 3),

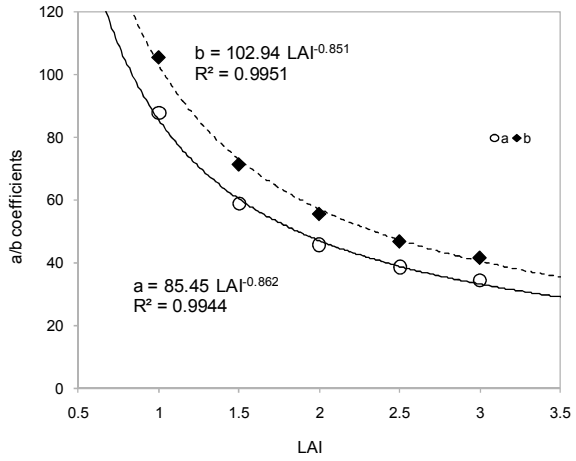

Figure 3. Relationship between LAI and the slope (a) and intercept (b) of the relationships between ρ750/ρ710 and different values of LAI.

Combining the regressions for *a* and *b* with equation (1), results in the following equation for the estimation of Ch_{a+b}:

$$Ch_{a+b} = (85.45 \times LAI^{-0.86})\frac{\rho 750}{\rho 710} - 102.94 \times LAI^{-0.85} \qquad (2)$$

The use of the reflectance ratio in combination with the LAI resulted in an improvement of the estimates of Ch_{a+b}. The regression of the input Ch_{a+b} against Ch_{a+b} calculated with equation (2) had an r^2=0.96 and RMSE=1.31µg/cm^2. In contrast, the results using the simple ρ750/710 ratio are r^2=0.32 and RMSE=5.5 µg/cm^2.

The analysis of the digital hemispherical photography (DHP) showed a very good correlation between *fCover* and the effective LAI calculated with CANEye (figure 4). Additionally the validation of the *fCover* from the DHP and the fractional cover calculated with the LiDAR shows a r^2=0.4 and a slope very close to one (slope=1.028 and intercept=0.08, n=26). However, direct relationships between LAI from DHP and LiDAR derived indices like the ratio of returns from high and total point returns showed low correlation coefficients. This is due to the difficulties of getting high accuracy GPS readings within the forest. We suspected that the GPS position of the DHP stations may differ with the actual position where the images were taken.

The resulting map of effective LAI (figure 5) shows the heterogeneity in the area. The areas in the Northwest have recently been partially logged and have lower LAI while the areas in the Northeast with higher values of LAI are undisturbed.

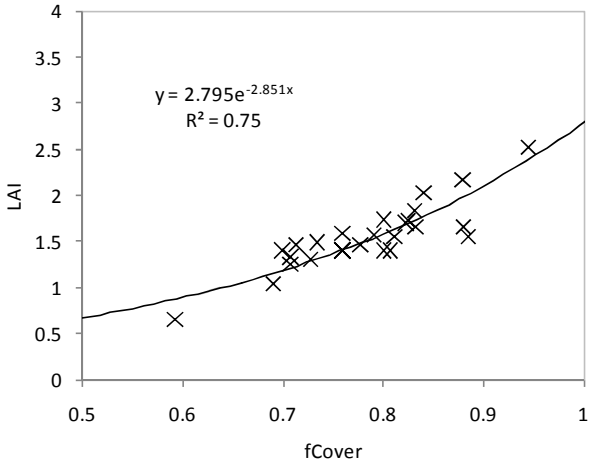

Figure 4. Relationship between the fractional cover (fCover) and the leaf area index (LAI) for the different stations of the hemispherical photos (n=26).

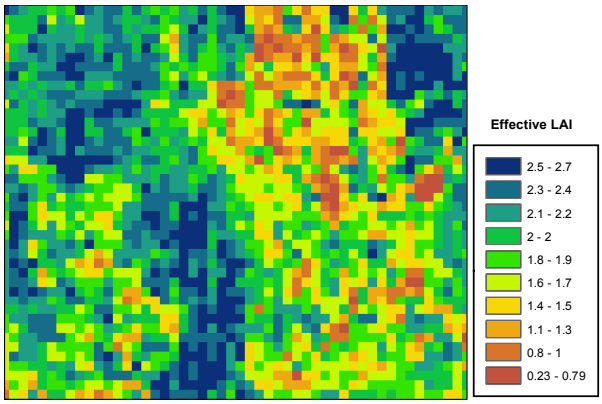

Figure 5. Map of effective LAI calculated from the LiDAR data and scaled to 100m of grid size.

A map of Ch_{a+b} (not shown) was calculated combining the map of LAI from the LiDAR and the ρ750/ρ710 reflectance ratio from the hyperspectral imagery using the equation (2). We used a simple linear relationship (, derived from leaf level measurements, to scale from Chl_{a+b} to $V_{cmax,0}$. Figure 6 shows the map of $V_{cmax,0}$ with 100m of grid size. The pattern is very similar to the distribution of LAI and the areas that have been recently logged show also lower chlorophyll content. However, we noticed that some areas that were partially logged some years ago and have grassy understorey, have low levels of Ch_{a+b}.. The cause for this is that the simulations were done with a given fractional cover (0.7) and bare soil as background. A more elaborated set of simulations with a wider range of fCover

and background reflectances will likely improve these results.

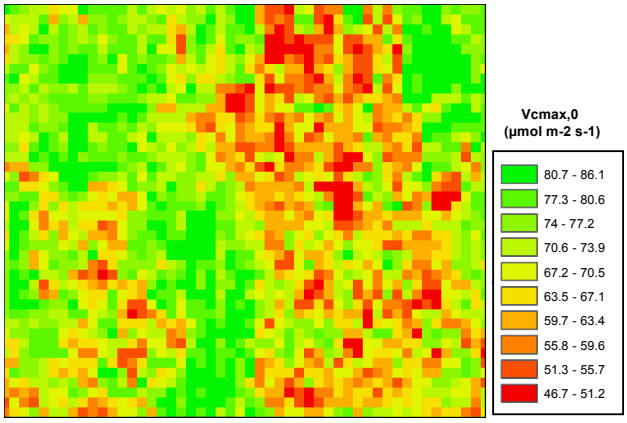

Figure 6. Map of $V_{cmax,0}$ calculated from the chlorophyll content and scaled to 100m grid size.

CABLE-SLI estimated CO_2 fluxes at the 2.392 grid elements using LAI and $V_{cmax,0}$ as spatially variable inputs while the rest of the parameters were set to their default values. The resulting map (figure 7) of net ecosystem exchange (NEE) shows a similar pattern as the LAI and $V_{cmax,0}$ maps, with negative values where the light interception and photosynthetic capacity are higher while there are areas around the logging patches where the NEE is positive (i.e. where CO_2 is released into the atmosphere).

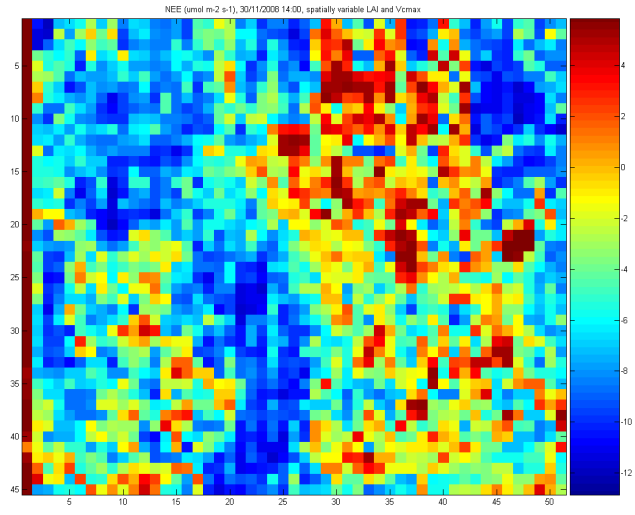

Figure 7. Net ecosystem exchange (NEE) calculated with CABLE-SLI using the maps of LAI and Vcmax,0 as input parameters.

CONCLUSIONS AND OUTLOOK

A combination of radiative transfer modelling and LiDAR and hyperspectral imagery allows for independent estimates of biophysical parameters like LAI and pigment concentration. Fused airborne LiDAR an hyperspectral data therefore have the advantage that, given that they base on completely different physical principles, can be used to constrain each other. Traditionally the problem of passive remote sensing has been scaling from leaf level to canopy and dealing with the structural effects in the reflectance. In this case, the radiative transfer models can account for the effects of the structure and allow developing relationships where structural parameters like LAI or fCover are inputs in the same way as the reflectance is.

Validation of the preliminary results shown in this communication is required. The validation will be performed at different scales and along the steps outlined in the methodology presented here.

The use of maps of the input parameters that drives the land surface models is a very valuable tool when it comes to understanding the effects of heterogeneity of the underlying landscape in the observations of eddy covariance towers. The combination of spatial based techniques with the right space-temporal scaling methodologies like footprint modelling and sensibility analysis (van Gorsel et al, these proceedings) will be something done routinely in the future.

REFERENCES

Baldocchi, D. D. (2003) "Assessing the eddy covariance technique for evaluating carbon dioxide exchange rates of ecosystems: past, present and future." Global Change Biology, 9, 479-492.

Barry, K.M, Newham, G, Stone, C. (2009) Estimation of chlorophyll content in Eucalyptus globolous foliage with the leaf reflectance model PROSPECT" AgForMet, 149, 1209-1213

BCAL LiDAR Tools. Boise Center Aerospace Laboratory. Idaho State University. (Last visited 4 Feb 2011): http://bcal.geology.isu.edu/Envitools.shtml

Feret, JB, François, C, Asner, GP, Gitelson, AA., Martin, RE, Bidel, LPR., et al. (1998). PROSPECT 4 and 5: advances in the leaf optical properties model separating photosynthetic pigments. Remote Sensing of Environment, 112, 3030−3043

Gueymard, C.A. (2001). "Parameterized Transmittance Model for Direct Beam and Circumsolar Spectral Irradiance." Solar Energy (71:5); pp. 325-346.

North, PRJ, "Three-dimensional forest light interaction model using a Monte Carlo method." IEEE TGRS, 34(4), 946– 956, 1996.

Running, SW, Baldocchi, DD, Turner, D et al. A global terrestrial monitoring network, scaling tower fluxes with ecosystem modelling and EOS satellite data. Remote Sensing Environment, 70, 108-127, (1999)

Weiss, M, Baret, F, Smith GJ, Jonckheere, I, Coppin, P, (2004). Part II. Estimation of LAI, errors and sampling. Agricultural and Forest Meteorology 121 37–53

Zarco-Tejada, PJ, Miller, JR Mohammed, GH, Noland, TL, Sampson, PH. Scaling-up and Model Inversion methods with narrow-band Optical Indices for Chlorophyll Content Estimation in closed Forest Canopies with Hyperspectral Data. IEEE TGRS, 39(7), 1491-1507, 2001

ACKNOWLEDGEMENTS

This work was supported by the Australian Greenhouse Office through the Australian Climate Change Science Program. We thank State Forests of NSW for permission to install experimental equipment in Bago Maragle State Forests. We also acknowledge contributions to this work by Gael Picoulet, Jenny Lovell, David Jupp, David Colville. Many thanks go to Shakti and Jorg Hacker for airborne data acquisition and processing support. Jose A.J. Berni is funded by a Postdoctoral Fellowship from the Ministerio de Educacion (Spain).